Improved genome assembly and annotation for the rock pigeon (*Columba livia*)

Carson Holt[*,†], Michael Campbell[*,1], David A. Keays[‡], Nathaniel Edelman[‡,2], Aurélie Kapusta[*,†], Emily Maclary[§], Eric Domyan[§,**], Alexander Suh[††], Wesley C. Warren[‡‡], Mark Yandell[*,†], M. Thomas P. Gilbert[§§,***], Michael D. Shapiro[§]

* Department of Human Genetics, University of Utah, Salt Lake City, UT, USA

† USTAR Center for Genetic Discovery, University of Utah, Salt Lake City, UT, USA

‡ Research Institute of Molecular Pathology, Vienna, Austria

§ Department of Biology, University of Utah, Salt Lake City, UT, USA

** Department of Biology, Utah Valley University, Orem, UT, USA

†† Department of Evolutionary Biology (EBC), University of Uppsala, Uppsala, Sweden

‡‡ Genome Institute at Washington University, St. Louis, MO, USA

§§ Natural History Museum of Denmark, University of Copenhagen, Copenhagen, Denmark

*** Norwegian University of Science and Technology, University Museum, 7491 Trondheim, Norway

1 Current address: Division of Plant Biology, Cold Spring Harbor Laboratory, Cold Spring Harbor, NY, USA

2 Current address: Department of Organismic and Evolutionary Biology, Harvard University, Cambridge, MA, USA

Accession numbers:

BioProject: PRJNA167554

Genome: This Whole Genome Shotgun project has been deposited at DDBJ/ENA/GenBank under the accession AKCR00000000. The version described in this paper is version AKCR02000000.

RNAseq data: SAMN07417936, SAMN07417937, SAMN07417938, SAMN07417939, SAMN07417940, SAMN07417941, SAMN07417942, SAMN07417943

Running title:

"HiRise genome assembly of rock pigeon"

Keywords:

Columba livia, rock pigeon, HiRise assembly, MAKER annotation

Author for Correspondence:

Michael D. Shapiro, Department of Biology, University of Utah, 257 S 1400 E, Salt Lake City, UT 84108, shapiro@biology.utah.edu, +1 801 581 5690

ABSTRACT

The domestic rock pigeon (*Columba livia*) is among the most widely distributed and phenotypically diverse avian species. This species is broadly studied in ecology, genetics, physiology, behavior, and evolutionary biology, and has recently emerged as a model for understanding the molecular basis of anatomical diversity, the magnetic sense, and other key aspects of avian biology. Here we report an update to the *C. livia* genome reference assembly and gene annotation dataset. Greatly increased scaffold lengths in the updated reference assembly, along with an updated annotation set, provide improved tools for evolutionary and functional genetic studies of the pigeon, and for comparative avian genomics in general.

INTRODUCTION

Intensive selective breeding of the domestic rock pigeon (*Columba livia*) has resulted in over 350 breeds with extreme differences in morphology and behavior (Levi 1986; Domyan and Shapiro 2017). The large phenotypic differences among different breeds make them a useful model for studying the genetic basis of radical phenotypic changes, which are more typically found among different species rather than within a single species.

In genetic and genomic studies of *C. livia*, linkage analysis is important for identifying genotypes associated with specific phenotypic traits of interest (Domyan and Shapiro 2017); however, short scaffold sizes in the Cliv_1.0 draft reference assembly (Shapiro et al. 2013) hinder computationally-based comparative analyses. Short scaffolds also make

63 it more difficult to identify structural changes, such as large insertions or deletions, that
64 are responsible for traits of interest (Domyan et al. 2014; Kronenberg et al. 2015).
65
66 Here we present the Cliv_2.1 reference assembly and an updated gene annotation set. The
67 new assembly greatly improves scaffold length over the previous draft reference
68 assembly, and updated gene annotations show improved concordance with both
69 transcriptome and protein homology evidence.
70

71 MATERIALS & METHODS

72 Genome sequencing and assembly

73 Genomic DNA from a female Danish tumbler pigeon (full sibling of the male bird used
74 for the original Cliv_1.0 assembly (Shapiro et al. 2013)) was extracted from blood using
75 a modified "salting out" protocol (Miller et al. 1988; modifications from
76 http://www.protocol-online.org/prot/Protocols/Extraction-of-genomic-DNA-from-whole-
77 blood-3171.html, accessed 06 February 2018)). Blood was frozen immediately after
78 collection and stored at -80°C, and purified DNA was resuspended in 10 mM Tris-HCl.
79 The sample went through 2 freeze-thaw cycles before being used to construct the libraries
80 described below.
81
82 Extracted DNA was used to produce long-range sequencing libraries using the "Chicago"
83 method (Putnam et al. 2016) by Dovetail Genomics (Santa Cruz, CA). Two Chicago
84 libraries were prepared and sequenced on the Illumina HiSeq platform to a final physical
85 coverage (1-50 kb pairs) of 390x.

86

87 Scaffolding was performed by Dovetail Genomics using HiRise assembly software and
88 the Cliv_1.0 assembly as input. Briefly, Chicago reads were aligned to the input assembly
89 to identify and mask repetitive regions, and then a likelihood model was applied to
90 identify mis-joins and score prospective joins for scaffolding. The final assembly was
91 then filtered for length and gaps according to NCBI submission specifications.

92

93 **Custom repeat library**

94 A repeat library for *C. livia* was built by combining libraries from existing avian species
95 (Zhang et al. 2014a) together with repeats identified *de novo* for the Cliv_2.1 assembly.
96 *De novo* repeat identification was performed using RepeatScout (Price et al. 2005) with
97 default parameters (>3 copies) to generate consensus repeat sequences. Identified repeats
98 with greater than 90% sequence identity and a minimum overlap of 100 bp were
99 assembled using Sequencher (Yokouchi et al. 1993). Repeats were classified into
100 transposable element (TE) families using multiple lines of evidence, including homology
101 to known elements, presence of terminal inverted repeats (TIRs), and detection of target
102 site duplications (TSDs). Homology-based evidence was obtained using RepeatMasker
103 (Smit et al. 1996), as well as the homology module of the TE classifying tool RepClass
104 (Feschotte et al. 2009). RepClass was also used to identify signatures of transposable
105 elements (TIRs, TSDs). We then eliminated non-TE repeats (simple repeats or gene
106 families), using custom Perl scripts (available at https://github.com/4ureliek/ReannTE).

107

108 In our custom repeat analysis, using the script ReannTE_FilterLow.pl, consensus
109 sequences were labeled as simple repeats or low complexity repeats if 80% of their length
110 could be annotated as such by RepeatMasker (the library was masked with the option -
111 noint). Next using the ReannTE_Filter-mRNA.pl script, consensus sequences were
112 compared to RefSeq (Pruitt et al. 2007) mRNAs (as of March 7th 2016) with TBLASTX
113 (Altschul et al. 1990). Sequences were eliminated from the library when: (i) the e-value
114 of the hit was lower than 1E-10; (ii) the consensus sequence was not annotated as a TE;
115 and (iii) the hit was not annotated as a transposase or an unclassified protein. The script
116 ReannTE_MergeFasta.pl was then used to merge our library with a library combining
117 RepeatModeler (Smit and Hubley 2008) outputs from 45 bird species (Kapusta et al.
118 2017) and complemented with additional avian TE annotations (International Chicken
119 Genome Sequencing 2004; Warren et al. 2010; Bao et al. 2015). Merged outputs were
120 then manually inspected to remove redundancy, and all DNA and RTE class transposable
121 elements were removed and replaced with manually curated consensus sequences, which
122 were either newly (DNA elements) or previously generated (RTEs) (Suh et al. 2016).
123
124 **Repeat landscape**
125 We used RepeatMasker software v4.0.7 (Smit et al. 2015) and our custom library to
126 annotate the repeats in Cliv_2.1. RepeatMasker was run with the NCBI/RMBLAST
127 v2.6.0+ search engine (-e ncbi), the sensitive (-s) option, the -a option in order to obtain
128 the alignment file, and without RepeatMasker default libraries. We then used the
129 parseRM.pl script v5.7 (available at https://github.com/4ureliek/Parsing-RepeatMasker-
130 Outputs (Kapusta et al. 2017)), on the alignment files from Repeat Masker, with the -l

131 option and a substitution rate of 0.002068 substitutions per site per million years (Zhang
132 et al. 2014b). The script collects the percentage of divergence to the consensus for each
133 TE fragment, after correction for higher mutation rate at CpG sites and the Kimura 2-
134 Parameter divergence metric (provided in the alignment files from RepeatMasker).
135 The percentage of divergence to the consensus is a proxy for age (the older the TE
136 invasion, the more mutations will accumulate in TE fragments), to which the script
137 applies the substitution rate in order to split TE fragments into bins of 1 My.
138
139 **Transcriptomics**
140 RNA was extracted from adult tissues (brain, retina, subepidermis, cochlear duct, spleen,
141 olfactory epithelium) of the racing homer breed, and one whole embryo each of a racing
142 homer and a parlor roller (approximately embryonic stage 25 (Hamburger and Hamilton
143 1951)). RNA-seq libararies were prepared and sequenced using 100-bp paired-end
144 sequencing on the Illumina HiSeq 2000 platform at the Research Institute of Molecular
145 Pathology, Vienna (adult tissues), and the Genome Institute at Washington University, St.
146 Louis (embryos). RNA-seq data generated for the Cliv_1.0 annotation were also
147 downloaded from the NCBI public repository for *de novo* re-assembly. Accession
148 numbers for these public data are SRR521357 (Danish tumbler heart), SRR521358
149 (Danish tumbler liver), SRR521359 (Oriental frill heart), SRR521360 (Oriental frill
150 liver), SRR521361 (Racing homer heart), and SRR521362 (Racing homer liver).
151
152 Each FASTQ file was processed with FastQC (http://www.bioinformatics.babraham.ac.
153 uk/projects/fastqc/) to assess quality. When FastQC reported overrepresentation of

154 Illumina adapter sequences, we trimmed these sequences with fastx_clipper from the
155 FASTX-Toolkit (http://hannonlab.cshl.edu/fastx_toolkit/). We used FASTX-Toolkit for
156 two additional functions: runs of low quality bases at the start of reads were trimmed with
157 fastx_trimmer when necessary (quality cutoff of -Q 33), and reads were then trimmed
158 with fastq_quality_trimmer (-Q 33). Finally, each pair of sequence files was assembled
159 with Trinity (Grabherr et al. 2011) version r20131110 using the --jaccard_clip option.
160

161 **Genome annotation**

162 The pre-existing reference Gnomon (Souvorov et al. 2010) derived gene models for the
163 Cliv_1.0 assembly (GCA_000337935.1) were mapped onto the updated Cliv_2.1
164 reference assembly using direct alignment of transcript FASTA entries. This was done
165 using the alignment workflow of the genome annotation pipeline MAKER (Cantarel et al.
166 2008; Holt and Yandell 2011), which first seeds alignments using BLASTN (Altschul et
167 al. 1990) and then polishes the alignments around splice sites using Exonerate (Slater and
168 Birney 2005). Results were then filtered to remove alignments that had an overall match
169 of less than 90% of the original model (match is calculated as percent identity multiplied
170 by percent end-to-end coverage).
171

172 For final annotation, MAKER was allowed to identify *de novo* gene models that did not
173 overlap the aligned Gnomon models. Protein evidence sets used by MAKER included
174 annotated proteins from *Pterocles gutturalis* (yellow-throated sandgrouse) (Zhang et al.
175 2014a) and *Gallus gallus* (chicken) (International Chicken Genome Sequencing 2004)
176 together with all proteins from the UniProt/Swiss-Prot database (Bairoch and Apweiler

177 2000; UniProt 2007). The transcriptome evidence sets for MAKER included Trinity
178 mRNA-seq assemblies from multiple *C. livia* breeds and tissues (methods for
179 transcriptome assembly are described above). Gene predictions were produced within
180 MAKER by Augustus (Stanke and Waack 2003; Stanke et al. 2008). Augustus was
181 trained using 1000 Cliv_1.0 Gnomon gene models that were split using the
182 randomSplit.pl script into sets for training and evaluation. We followed a semi-automatic
183 training protocol
184 (https://vcru.wisc.edu/simonlab/bioinformatics/programs/augustus/docs/tutorial2015/train
185 ing.html, accessed 9 February 2018). Repetitive elements in the genome were identified
186 using the custom repeat library described above.
187
188 **Linkage map construction and anchoring to current assembly**
189 Genotyping by sequencing (GBS) data was generated, trimmed, and filtered as previously
190 described (Domyan et al. 2016). Reads were mapped to the Cliv_2.1 assembly using
191 Bowtie2 (Langmead and Salzberg 2012). Genotypes were called using Stacks (Catchen et
192 al. 2011), with a minimum read-depth cutoff of 10. Thresholds for automatic corrections
193 were set using the parameters –min_hom_seqs 10, –min_het_seqs 0.01, –max_het_seqs
194 0.15. Sequencing coverage and genotyping rate varied between individuals, and birds
195 with genotyping rates in the bottom 25% were excluded from map assembly.
196
197 Genetic map construction was performed using R/qtl v1.41-6 (www.rqtl.org) (Broman et
198 al. 2003). For autosomal markers, markers showing segregation distortion (Chi-square, p
199 < 0.01) were eliminated. Sex-linked scaffolds were assembled and ordered separately,

200 due to differences in segregation pattern for the Z-chromosome. Z-linked scaffolds were
201 identified by assessing sequence similarity and gene content between pigeon scaffolds
202 and the Z-chromosome of the annotated chicken genome (Ensembl Gallus_gallus-5.0).
203
204 Pairwise recombination fractions were calculated for all autosomal and Z-linked markers.
205 Missing data were imputed using "fill.geno" with the method "no_dbl_XO". Duplicate
206 markers were identified and removed. Within individual scaffolds, R/qtl functions
207 "droponemarker" and "calc.errorlod" were used to assess genotyping error. Markers were
208 removed if dropping the marker led to an increased LOD score, or if removing a non-
209 terminal marker led to a decrease in length of >10 cM that was not supported by physical
210 distance. Individual genotypes were removed if they showed with error LOD scores >5
211 (Lincoln and Lander 1992). Linkage groups were assembled from 2960 autosomal
212 markers and 232 Z-linked markers using the parameters (max.rf 0.1, min.lod 6). In the
213 rare instance that single scaffolds were split into multiple linkage groups, linkage groups
214 were merged if supported by recombination fraction data; these instances typically
215 reflected large physical gaps between markers on a single scaffold. Scaffolds in the same
216 linkage group were manually ordered based on calculated recombination fractions and
217 LOD scores.
218
219 To compare the linkage map to the original genome assembly (Cliv_1.0), each 90-bp
220 locus containing a genetic marker was parsed from the Stacks output file
221 "catalogXXX_tags.tsv" and queried to the Cliv_1.0 assembly using BLASTN (v2.6.0+)
222 with the parameters –max_target_seqs 1 –max hsps 1. 3175 of the 3192 loci (99.47%)

223 from the new assembly had a BLAST hit with an E-value < 4e-24 and were retained.

224

225 **Assembly comparisons**

226 FASTA files from the Cliv_2.1 and colLiv2 (Damas et al. 2017) genome assemblies were
227 hard masked using NCBI WindowMasker (Morgulis et al. 2006) and genome-wide
228 alignments were calculated with LAST (Kielbasa et al. 2011). From these alignments, a
229 genome-scale dotplot indicating syntenic regions was generated using SynMap (Lyons
230 and Freeling 2008; Lyons et al. 2008).

231

232 The colLiv2 assembly is currently unannotated. Therefore, to compare gene content
233 between assemblies, we estimated the number of annotated Cliv_2.1 genes absent from
234 colLiv2 based on gene coordinates. Based on the length of LAST alignments, we
235 calculated the percent of each Cliv_2.1 scaffold aligning to colLiv2. Scaffolds were
236 divided into four groups based on alignments: Cliv_2.1 scaffolds that did not align to
237 colLiv2, Cliv_2.1 scaffolds where LAST alignments to colLiv2 covered less than 50% of
238 the total scaffold length, Cliv_2.1 scaffolds where LAST alignments to colLiv2 covered
239 between 50% and 75% of the total scaffold length, and Cliv_2.1 scaffolds where LAST
240 alignments to colLiv2 covered 75% or more of the total scaffold length. For each of these
241 groups, the number of scaffolds containing genes was quantified. Many of these scaffolds
242 are small, and some may be missing entirely or in part from the alignment due to masking
243 of repetitive elements. If annotated gene coordinates from Cliv_2.1 scaffolds fell partially
244 or entirely within a region aligned to colLiv2, these genes were considered “present” in
245 colLiv2. Thus, the number of genes marked as “absent” in colLiv2 might be a

246 conservative estimate.

247

248 To compare the linkage map to colLiv2, each 90-bp locus containing a genetic marker

249 was parsed from the Stacks output file "catalogXXX_tags.tsv" and queried to the colLiv2

250 assembly using BLASTN (v2.6.0+) with the parameters –max_target_seqs 1 –max hsps

251 1.

252

253 **Data availability**

254 This Whole Genome Shotgun project has been deposited at DDBJ/ENA/GenBank under

255 the accession AKCR00000000. The version described in this paper is version

256 AKCR02000000. The Cliv_2.1 assembly, annotation, and associated data are available at

257 ftp://ftp.ncbi.nlm.nih.gov/genomes/all/GCA/000/337/935/GCA_000337935.2_Cliv_2.1.

258 RNA-seq data are deposited in the SRA database with the BioSample accession numbers

259 SAMN07417936-SAMN07417943, and sequence accessions SRR5878849-

260 SRR5878856. Assembly and RNA-seq data are publicly available in NCBI databases

261 under BioProject PRJNA167554. File S1 contains Tables S1-S7. Files S2 and S3 contain

262 recombination fraction data used to construct Figures 4a and 4b, respectively.

263

264 **RESULTS AND DISCUSSION**

265 **Genome assembly**

266 The final Cliv_2.1 reference assembly is 1,108,534,737 base pairs in length and consists

267 of 15,057 scaffolds (Table 1). A total of 1,015 scaffolds contain a gene annotation.

268 Completion analysis of the assembly using BUSCO v2 and the odb9 Vertebrata ortholog

269 dataset (Simao et al. 2015) suggests that Cliv_2.1 is 72.9 (assembly) to 86.2%
270 (annotation) complete. These statistics are nearly identical to the Cliv_1.0 assembly
271 estimate of 72.3-86.4% (Table 2); therefore, we found no significant changes to
272 completeness between the two assemblies. The Chicago libraries and HiRise assembly
273 were designed to improve scaffolding of the original assembly, not to fill gaps, so we did
274 not expect substantial improvement to assembly completeness in Cliv_2.1. The major
275 improvement to the Cliv_2.1 assembly is rather an increase in scaffold length (Fig. 1a).
276 Overall, the N50 scaffold length increased to 14.3 megabases compared to 3.15
277 megabases for the previous reference assembly, a greater than 4-fold increase.
278
279 The new assembly joins scaffolds that we knew were adjacent but were separated
280 previously (see Table S1 for full catalog of positions of the original assembly in the new
281 assembly, and Table S2 for full catalog of breaks in the original assembly to form the
282 new assembly). For example, we previously determined that Cliv_1.0 Scaffolds 70 and
283 95 were joined based on genetic linkage data from a laboratory cross (Domyan et al.
284 2016). These two sequences are now joined into a single scaffold in the Cliv_2.1
285 assembly (see Table S3 for positions of genetic markers in Cliv_1.0 and Cliv_2.1). At
286 least one gene model (RefSeq LOC102093126), which was previously split across two
287 contigs, has now been unified into a single model on a single scaffold.
288
289 **Repeat landscape**
290 With our custom library, we identified 8.04% (89.1 Mb; Table S3) of the genome
291 assembly as repeats, which is slightly higher than the previously published estimates of

292 7.25% (Zhang et al. 2014b) and 7.83% (Kapusta and Suh 2017). To illustrate the
293 temporal dynamics of TE accumulation (see Methods), we split the amount of DNA of
294 each TE class by bins of 1 million years (My) (Fig. 2). This landscape shows that TE
295 accumulation has been consistent throughout time, with potentially some recently active
296 elements. This includes CR1 LINEs (part of the non-LTR fraction), which are presumed
297 to be inactive in most birds (Kapusta and Suh 2017), but comprise over 0.1 Mb of CR1
298 copies in the youngest bin (0-1 My) in the Cliv_2.1 assembly (Table S4).
299
300 **Transcriptome assemblies**
301 A total of 1,936,543 transcripts were assembled from the 14 RNA-seq data sets. Numbers
302 of assembled transcripts from each tissue are listed in Table S3. BUSCO analysis
303 indicated 85.6% completeness of the union of transcriptome assemblies compared to the
304 Vertebrata ortholog set.
305
306 **Annotation**
307 The updated annotation set contains 15,392 gene models encoding 18,966 transcripts
308 (Table 4). This represents only a minor update of the reference annotation set as 94.7% of
309 previous models were mapped forward nearly unmodified (90% exact match for 14,898
310 out of 15,724 previous gene models) and only 494 new gene models were added to the
311 Cliv_2.1 annotation set (Table 5).
312
313 The updated annotation set shows a modest improvement in concordance with aligned
314 evidence datasets from mRNA-seq and cross species protein homology evidence relative

315 to the Cliv_1.0 set as measured by Annotation Edit Distance (AED) (Eilbeck et al. 2009;
316 Holt and Yandell 2011). As a result, transcript models in the Cliv_2.1 annotation tend to
317 have lower AED values than the Cliv_1.0 set (Figure 2; the cumulative distribution
318 function (CDF) curve is shifted to the left). Lower AED values indicate greater model
319 concordance with aligned transcriptome and protein homology data. Furthermore, the
320 Cliv_2.1 dataset displays greater transcript counts in every AED bin despite having
321 slightly fewer transcripts overall compared to the Cliv_1.0 dataset (Table S3). The higher
322 bin counts indicate that lower AED values are not solely a result of removing
323 unsupported models from the annotation set, but rather suggest that evidence
324 concordance has improved overall.
325
326 **Linkage map**
327 The linkage map consists of 3192 markers assembled into 48 autosomal linkage groups
328 and a single Z-chromosome linkage group (Table S5. The map contains markers from
329 236 scaffolds. Together, these scaffolds encompass 1,048,536,443 bp, or 94.6% of the
330 Cliv_2.1 assembly, and include 13026 of 15392 annotated genes (84.6%). Cliv_2.1
331 scaffolds are strongly supported by linkage data. For 235 out of 236 scaffolds included in
332 the linkage map, all GBS markers mapped to that scaffold form a single contiguous block
333 within one linkage group (scaffold ScoHet5_252 was split between 2 linkage groups).
334 Additionally, within-scaffold marker order was largely supported by calculated pairwise
335 recombination fractions.
336
337 **Comparison with colLiv2 genome assembly**

338 Recently, Damas et al. (2017) used computational methods and universal avian bacterial
339 artificial chromosome (BAC) probes to achieve chromosome-level scaffolding using the
340 Cliv_1.0 assembly as input material. This assembly, named colLiv2 (GenBank assembly
341 accession GCA_001887795.1; 1,018,016,946 bp in length), is approximately 8% smaller
342 than the Cliv_2.1 assembly.
343
344 Based on genome-wide pairwise alignments using LAST (Kielbasa et al. 2011), a
345 substantial number of regions of Cliv_2.1 that do not align to colLiv2 genome contain
346 both unique sequence and annotated genes. Based on gene coordinates, 1184 annotated
347 Cliv_2.1 genes were absent from colLiv2 (Table 6).
348
349 Of the 3192 GBS makers mapped to Cliv_2.1, 2940 markers (92.1%) mapped to colLiv2
350 with an E-value <4e-24. Of the remaining markers, 7 mapped to colLiv2 with an E-value
351 >4e-24, and 245 markers (7.67%) failed to map to colLiv2 entirely. We assessed the
352 agreement between marker and linkage data by calculating pairwise recombination
353 fractions for the 2940 markers, then plotted these recombination fractions in the order in
354 which markers appear on the colLiv2 chromosome-level scaffolds. Overall, the marker
355 order largely agrees with calculated recombination fractions; however, we identified a
356 number of locations where pairwise recombination fractions suggest that portions of the
357 colLiv2 chromosomes are not ordered properly, as exemplified in Fig. 5. We also
358 identified 42 markers for which the location with the best sequence match in colLiv2
359 appears to be incorrect based on recombination fraction estimates; these markers are
360 summarized in Table S7.

361

362 **Conclusions**

363 The improved scaffold lengths of Cliv_2.1, as well as the updated gene model
364 annotations, should further empower ongoing studies to identify genes responsible for
365 phenotypic traits of interest and improve detection of regions under selection due to
366 longer scaffolds. We also expect to be able to better identify large deletions and other
367 structural variants responsible for specific phenotypes now that they can be more clearly
368 mapped to longer scaffolds. Finally, the new transcriptomic data provides tissue-specific
369 expression profiles for several adult tissue types and an important embryonic stage for the
370 morphogenesis of limbs, craniofacial structures, skin, and other tissues.

371

372 **ACKNOWLEDGEMENTS**

373 We thank Dovetail Genomics for their aid in scaffolding the assembly; Julia Carleton and
374 Anna Vickrey for technical support; and Elena Boer for comments on the manuscript.
375 This work was supported by National Science Foundation grant DEB1149160 and
376 National Institutes of Health (NIH) grant R01GM115996 to MDS; NSF EAGER grant
377 IOS1561337 to MY; a European Research Council starting grant 336724 and Austrian
378 Science Fund (FWF) grant Y726 to DAK; and European Research Council Consolidator
379 grant 681396 to MTPG. We gratefully acknowledge research support from Boehringer
380 Ingelheim at the Research Institute of Molecular Pathology, and support and resources
381 from the Center for High Performance Computing at the University of Utah.

382

383

384 **REFERENCES**

385 Altschul, S. F., W. Gish, W. Miller, E. W. Meyers, and D. J. Lipman. 1990. Basic Local
386 Alignment Search Tool. Journal of Molecular Biology 215:403-410.
387 Bairoch, A. and R. Apweiler. 2000. The SWISS-PROT protein sequence database and
388 its supplement TrEMBL in 2000. Nucl. Acids Res. 28:45-48.
389 Bao, W., K. K. Kojima, and O. Kohany. 2015. Repbase Update, a database of repetitive
390 elements in eukaryotic genomes. Mob DNA 6:11.
391 Broman, K., H. Wu, S. Sen, and G. Churchill. 2003. R/qtl: QTL mapping in
392 experimental crosses. Bioinformatics 19:889-890.
393 Cantarel, B. L., I. Korf, S. M. C. Robb, G. Parra, E. Ross, B. Moore, C. Holt, A. Sanchez
394 Alvarado, and M. Yandell. 2008. MAKER: An easy-to-use annotation pipeline
395 designed for emerging model organism genomes. Genome Res. 18:188-196.
396 Catchen, J. M., A. Amores, P. Hohenlohe, W. Cresko, and J. H. Postlethwait. 2011.
397 Stacks: building and genotyping loci de novo from short-read sequences. G3
398 1:171-182.
399 Damas, J., R. O'Connor, M. Farre, V. P. E. Lenis, H. J. Martell, A. Mandawala, K. Fowler,
400 S. Joseph, M. T. Swain, D. K. Griffin, and D. M. Larkin. 2017. Upgrading short-
401 read animal genome assemblies to chromosome level using comparative
402 genomics and a universal probe set. Genome Res 27:875-884.
403 Domyan, E. T., M. W. Guernsey, Z. Kronenberg, S. Krishnan, R. E. Boissy, A. I. Vickrey,
404 C. Rodgers, P. Cassidy, S. A. Leachman, J. W. Fondon, 3rd, M. Yandell, and M. D.
405 Shapiro. 2014. Epistatic and combinatorial effects of pigmentary gene
406 mutations in the domestic pigeon. Curr Biol 24:459-464.
407 Domyan, E. T., Z. Kronenberg, C. R. Infante, A. I. Vickrey, S. A. Stringham, R. Bruders,
408 M. W. Guernsey, S. Park, J. Payne, R. B. Beckstead, G. Kardon, D. B. Menke, M.
409 Yandell, and M. D. Shapiro. 2016. Molecular shifts in limb identity underlie
410 development of feathered feet in two domestic avian species. eLife 5:e12115.
411 Domyan, E. T. and M. D. Shapiro. 2017. Pigeonetics takes flight: Evolution,
412 development, and genetics of intraspecific variation. Dev Biol 427:241-250.
413 Eilbeck, K., B. Moore, C. Holt, and M. Yandell. 2009. Quantitative measures for the
414 management and comparison of annotated genomes. BMC Bioinformatics
415 10:67.
416 Feschotte, C., U. Keswani, N. Ranganathan, M. L. Guibotsy, and D. Levine. 2009.
417 Exploring repetitive DNA landscapes using REPCLASS, a tool that automates
418 the classification of transposable elements in eukaryotic genomes. Genome
419 Biol Evol 1:205-220.
420 Grabherr, M. G., B. J. Haas, M. Yassour, J. Z. Levin, D. A. Thompson, I. Amit, X. Adiconis,
421 L. Fan, R. Raychowdhury, Q. Zeng, Z. Chen, E. Mauceli, N. Hacohen, A. Gnirke,
422 N. Rhind, F. di Palma, B. W. Birren, C. Nusbaum, K. Lindblad-Toh, N. Friedman,
423 and A. Regev. 2011. Full-length transcriptome assembly from RNA-Seq data
424 without a reference genome. Nature biotechnology 29:644-652.
425 Hamburger, V. and H. L. Hamilton. 1951. A series of normal stages in the
426 development of the chick embryo. Journal of Morphology 88:49-92.

427 Holt, C. and M. Yandell. 2011. MAKER2: an annotation pipeline and genome-
428 database management tool for second-generation genome projects. BMC
429 Bioinformatics 12:491.
430 International Chicken Genome Sequencing, C. 2004. Sequence and comparative
431 analysis of the chicken genome provide unique perspectives on vertebrate
432 evolution. Nature 432:695-716.
433 Kapusta, A. and A. Suh. 2017. Evolution of bird genomes-a transposon's-eye view.
434 Ann N Y Acad Sci 1389:164-185.
435 Kapusta, A., A. Suh, and C. Feschotte. 2017. Dynamics of genome size evolution in
436 birds and mammals. Proc Natl Acad Sci U S A 114:E1460-E1469.
437 Kielbasa, S. M., R. Wan, K. Sato, P. Horton, and M. C. Frith. 2011. Adaptive seeds tame
438 genomic sequence comparison. Genome Res 21:487-493.
439 Kronenberg, Z. N., E. J. Osborne, K. R. Cone, B. J. Kennedy, E. T. Domyan, M. D.
440 Shapiro, N. C. Elde, and M. Yandell. 2015. Wham: Identifying Structural
441 Variants of Biological Consequence. PLoS Comput Biol 11:e1004572.
442 Langmead, B. and S. L. Salzberg. 2012. Fast gapped-read alignment with Bowtie 2.
443 Nat Methods 9:357-359.
444 Levi, W. M. 1986. The Pigeon (Second Revised Edition). Levi Publishing Co., Inc.,
445 Sumter, S.C.
446 Lincoln, S. E. and E. S. Lander. 1992. Systematic detection of errors in genetic linkage
447 data. Genomics 14:604-610.
448 Lyons, E. and M. Freeling. 2008. How to usefully compare homologous plant genes
449 and chromosomes as DNA sequences. Plant J 53:661-673.
450 Lyons, E., B. Pedersen, J. Kane, M. Alam, R. Ming, H. Tang, X. Wang, J. Bowers, A.
451 Paterson, D. Lisch, and M. Freeling. 2008. Finding and comparing syntenic
452 regions among Arabidopsis and the outgroups papaya, poplar, and grape:
453 CoGe with rosids. Plant physiology 148:1772-1781.
454 Miller, S. A., D. D. Dykes, and H. F. Polesky. 1988. A simple salting out procedure for
455 extracting DNA from human nucleated cells. Nucleic Acids Res 16:1215.
456 Morgulis, A., E. M. Gertz, A. A. Schaffer, and R. Agarwala. 2006. WindowMasker:
457 window-based masker for sequenced genomes. Bioinformatics 22:134-141.
458 Price, A. L., N. C. Jones, and P. A. Pevzner. 2005. De novo identification of repeat
459 families in large genomes. Bioinformatics 21 Suppl 1:i351-358.
460 Pruitt, K. D., T. Tatusova, and D. R. Maglott. 2007. NCBI reference sequences
461 (RefSeq): a curated non-redundant sequence database of genomes,
462 transcripts and proteins. Nucleic Acids Res:D61 - 65.
463 Putnam, N. H., B. L. O'Connell, J. C. Stites, B. J. Rice, M. Blanchette, R. Calef, C. J. Troll,
464 A. Fields, P. D. Hartley, C. W. Sugnet, D. Haussler, D. S. Rokhsar, and R. E.
465 Green. 2016. Chromosome-scale shotgun assembly using an in vitro method
466 for long-range linkage. Genome Res 26:342-350.
467 Shapiro, M. D., Z. Kronenberg, C. Li, E. T. Domyan, H. Pan, M. Campbell, H. Tan, C. D.
468 Huff, H. Hu, A. I. Vickrey, S. C. Nielsen, S. A. Stringham, H. Hu, E. Willerslev, M.
469 T. Gilbert, M. Yandell, G. Zhang, and J. Wang. 2013. Genomic diversity and
470 evolution of the head crest in the rock pigeon. Science 339:1063-1067.

471 Simao, F. A., R. M. Waterhouse, P. Ioannidis, E. V. Kriventseva, and E. M. Zdobnov.
472 2015. BUSCO: assessing genome assembly and annotation completeness with
473 single-copy orthologs. Bioinformatics 31:3210-3212.
474 Slater, G. and E. Birney. 2005. Automated generation of heuristics for biological
475 sequence comparison. BMC Bioinformatics 6:31.
476 Smit, A. F. and R. Hubley. 2008. RepeatModeler Open-1.0
477 http://www.repeatmasker.org/.
478 Smit, A. F., R. Hubley, and P. Green. 1996. RepeatMasker Open-3.0
479 http://www.repeatmasker.org/.
480 Smit, A. F., R. Hubley, and P. Green. 2015. RepeatMasker Open-4.0.2013-2015
481 http://www.repeatmasker.org/.
482 Souvorov, A., Y. Kapustin, B. Kiryutin, V. Chetvernin, T. Tatusova, and D. Lipman.
483 2010. Gnomon – NCBI eukaryotic gene prediction tool. NCBI.
484 Stanke, M., M. Diekhans, R. Baertsch, and D. Haussler. 2008. Using native and
485 syntenically mapped cDNA alignments to improve de novo gene finding.
486 Bioinformatics 24:637-644.
487 Stanke, M. and S. Waack. 2003. Gene prediction with a hidden Markov model and a
488 new intron submodel. Bioinformatics 19:ii215-225.
489 Suh, A., C. C. Witt, J. Menger, K. R. Sadanandan, L. Podsiadlowski, M. Gerth, A.
490 Weigert, J. A. McGuire, J. Mudge, S. V. Edwards, and F. E. Rheindt. 2016.
491 Ancient horizontal transfers of retrotransposons between birds and
492 ancestors of human pathogenic nematodes. Nature communications 7:11396.
493 UniProt, C. 2007. The Universal Protein Resource (UniProt). Nucleic Acids Res:D193
494 - 197.
495 Warren, W. C., D. F. Clayton, H. Ellegren, A. P. Arnold, L. W. Hillier, A. Kunstner, S.
496 Searle, S. White, A. J. Vilella, S. Fairley, A. Heger, L. Kong, C. P. Ponting, E. D.
497 Jarvis, C. V. Mello, P. Minx, P. Lovell, T. A. Velho, M. Ferris, C. N. Balakrishnan,
498 S. Sinha, C. Blatti, S. E. London, Y. Li, Y. C. Lin, J. George, J. Sweedler, B.
499 Southey, P. Gunaratne, M. Watson, K. Nam, N. Backstrom, L. Smeds, B.
500 Nabholz, Y. Itoh, O. Whitney, A. R. Pfenning, J. Howard, M. Volker, B. M.
501 Skinner, D. K. Griffin, L. Ye, W. M. McLaren, P. Flicek, V. Quesada, G. Velasco, C.
502 Lopez-Otin, X. S. Puente, T. Olender, D. Lancet, A. F. Smit, R. Hubley, M. K.
503 Konkel, J. A. Walker, M. A. Batzer, W. Gu, D. D. Pollock, L. Chen, Z. Cheng, E. E.
504 Eichler, J. Stapley, J. Slate, R. Ekblom, T. Birkhead, T. Burke, D. Burt, C. Scharff,
505 I. Adam, H. Richard, M. Sultan, A. Soldatov, H. Lehrach, S. V. Edwards, S. P.
506 Yang, X. Li, T. Graves, L. Fulton, J. Nelson, A. Chinwalla, S. Hou, E. R. Mardis,
507 and R. K. Wilson. 2010. The genome of a songbird. Nature 464:757-762.
508 Yokouchi, Y., M. Yamamoto, T. Toyota, H. Sasaki, and A. Kuroiwa. 1993. Regulatory
509 interaction of positional signalings on coordinate expression of homeobox
510 genes in developing limb buds. Limb Development and Regeneration. Wiley-
511 Liss, Inc.
512 Zhang, G., B. Li, C. Li, M. T. Gilbert, E. D. Jarvis, J. Wang, and C. Avian Genome. 2014a.
513 Comparative genomic data of the Avian Phylogenomics Project. Gigascience
514 3:26.
515 Zhang, G., C. Li, Q. Li, B. Li, D. M. Larkin, C. Lee, J. F. Storz, A. Antunes, M. J. Greenwold,
516 R. W. Meredith, A. Odeen, J. Cui, Q. Zhou, L. Xu, H. Pan, Z. Wang, L. Jin, P.

517 Zhang, H. Hu, W. Yang, J. Hu, J. Xiao, Z. Yang, Y. Liu, Q. Xie, H. Yu, J. Lian, P.
518 Wen, F. Zhang, H. Li, Y. Zeng, Z. Xiong, S. Liu, L. Zhou, Z. Huang, N. An, J. Wang,
519 Q. Zheng, Y. Xiong, G. Wang, B. Wang, J. Wang, Y. Fan, R. R. da Fonseca, A.
520 Alfaro-Nunez, M. Schubert, L. Orlando, T. Mourier, J. T. Howard, G. Ganapathy,
521 A. Pfenning, O. Whitney, M. V. Rivas, E. Hara, J. Smith, M. Farre, J. Narayan, G.
522 Slavov, M. N. Romanov, R. Borges, J. P. Machado, I. Khan, M. S. Springer, J.
523 Gatesy, F. G. Hoffmann, J. C. Opazo, O. Hastad, R. H. Sawyer, H. Kim, K. W. Kim,
524 H. J. Kim, S. Cho, N. Li, Y. Huang, M. W. Bruford, X. Zhan, A. Dixon, M. F.
525 Bertelsen, E. Derryberry, W. Warren, R. K. Wilson, S. Li, D. A. Ray, R. E. Green,
526 S. J. O'Brien, D. Griffin, W. E. Johnson, D. Haussler, O. A. Ryder, E. Willerslev, G.
527 R. Graves, P. Alstrom, J. Fjeldsa, D. P. Mindell, S. V. Edwards, E. L. Braun, C.
528 Rahbek, D. W. Burt, P. Houde, Y. Zhang, H. Yang, J. Wang, E. D. Jarvis, M. T.
529 Gilbert and J. Wang. 2014b. Comparative genomics reveals insights into avian
530 genome evolution and adaptation. Science 346:1311-1320.
531

532 **FIGURES**

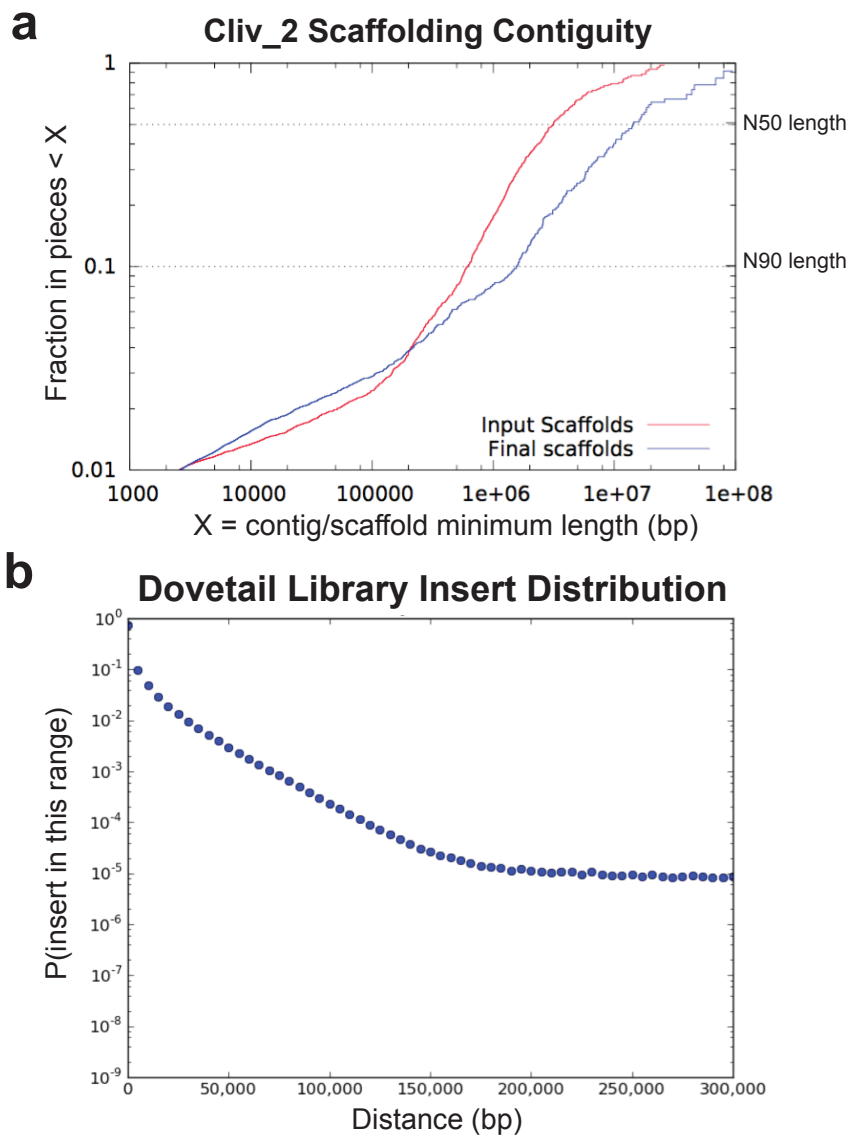

533

534 **Figure 1.** Assembly scaffolding contiguity and scaffolding library insert size

535 distributions. (a) Scaffolding comparison between Cliv_1.0 (input scaffolds) and Cliv_2.1

536 (final scaffolds) assemblies. (b) Distribution of Dovetail Genomics "Chicago" library

537 inserts.

538

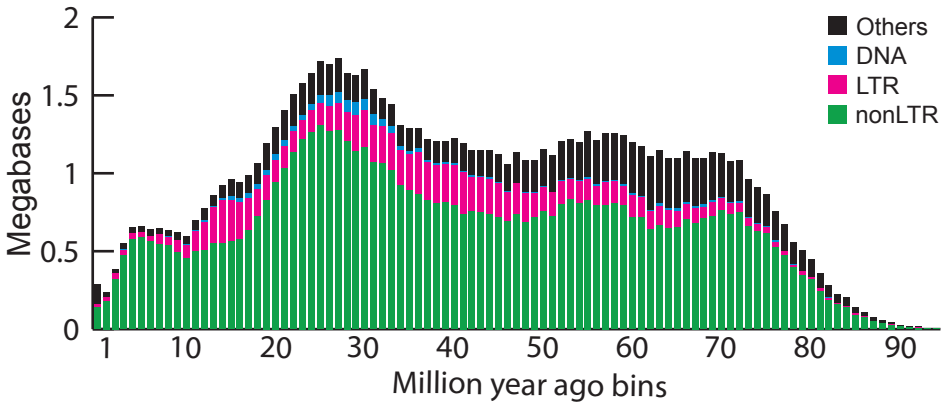

539

540 **Figure 2.** Temporal landscape of transposable elements. The amounts of DNA of each
541 TE class were split into bins of 1 My, shown on the x axis (see Methods). We note that
542 the lower detection of older elements (right of the graph) comes from a combination of
543 lack of detection and TE removal, and that the amount of DNA corresponding to recent
544 elements may be underestimated (recent copies are often collapsed in assemblies). The
545 "Others" category primarily includes unclassified repeats.

546

547

548

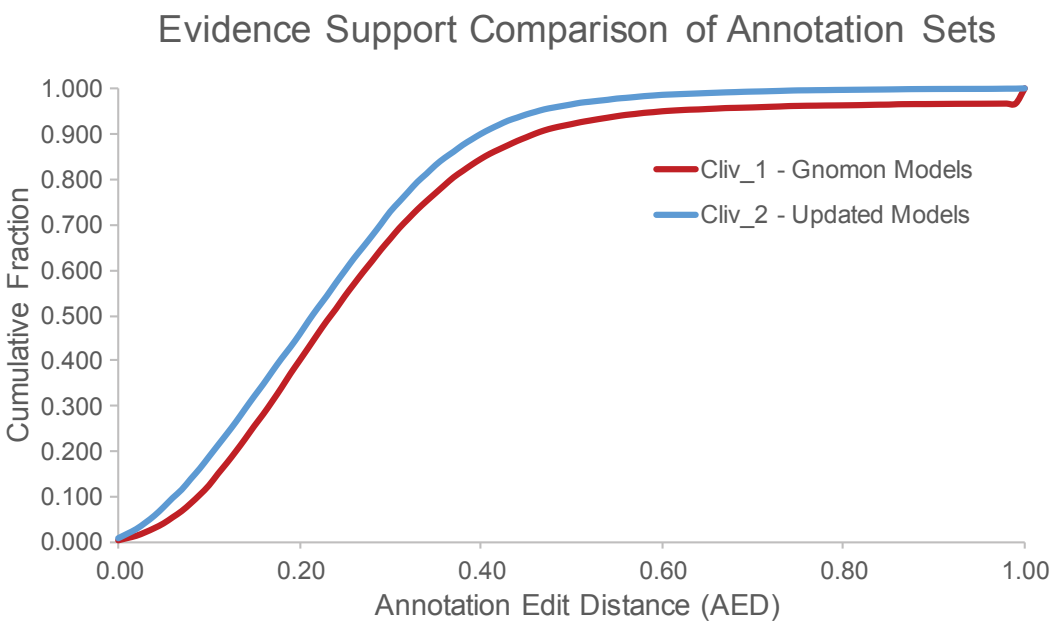

549

550

551 **Figure 3.** Evidence support comparison of annotation sets. Annotation edit distance

552 (AED) support for gene models in Cliv_2.1 (blue line) is improved over Cliv_1.0 (NCBI

553 Gnomon annotation, red line).

554

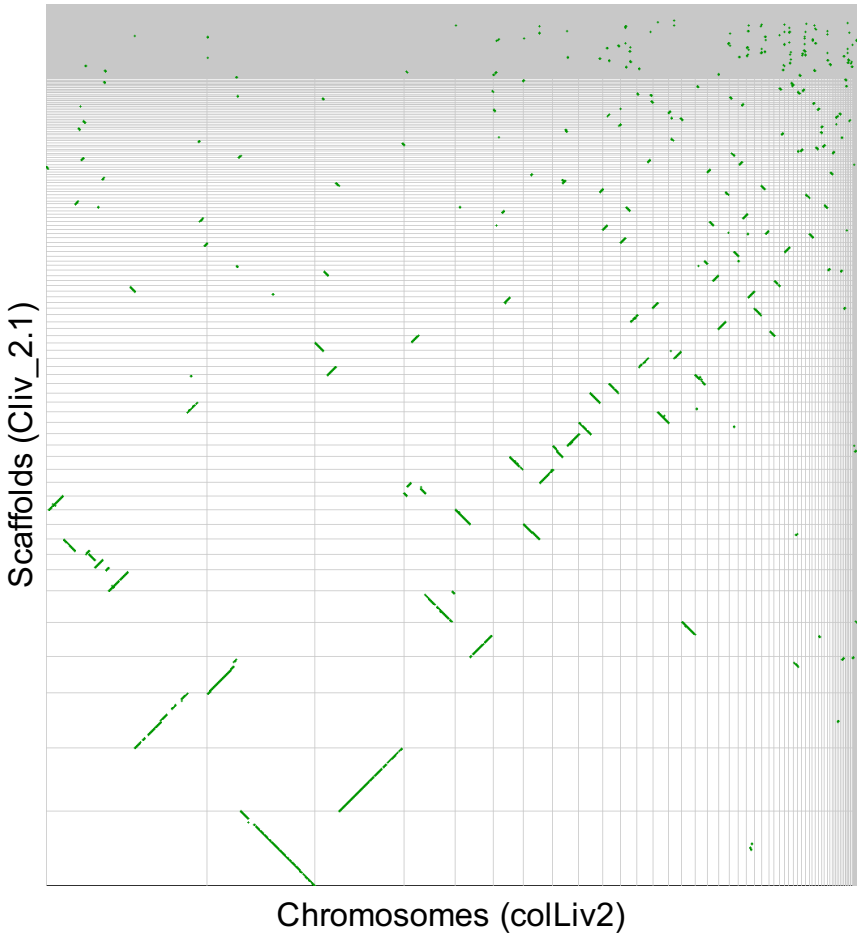

555

556

557 **Figure 4.** Dot plot of syntenic regions between the Cliv_2.1 and colLiv2 assemblies of

558 the *C. livia* genome. Each segment of the X axis represents a single colLiv2 scaffold

559 ordered from largest (left) to smallest (right), while each segment of the Y axis represents

560 a scaffold of the Cliv_2.1 assembly, ordered from largest (bottom) to smallest (top).

561 Green dots indicate aligned regions of synteny.

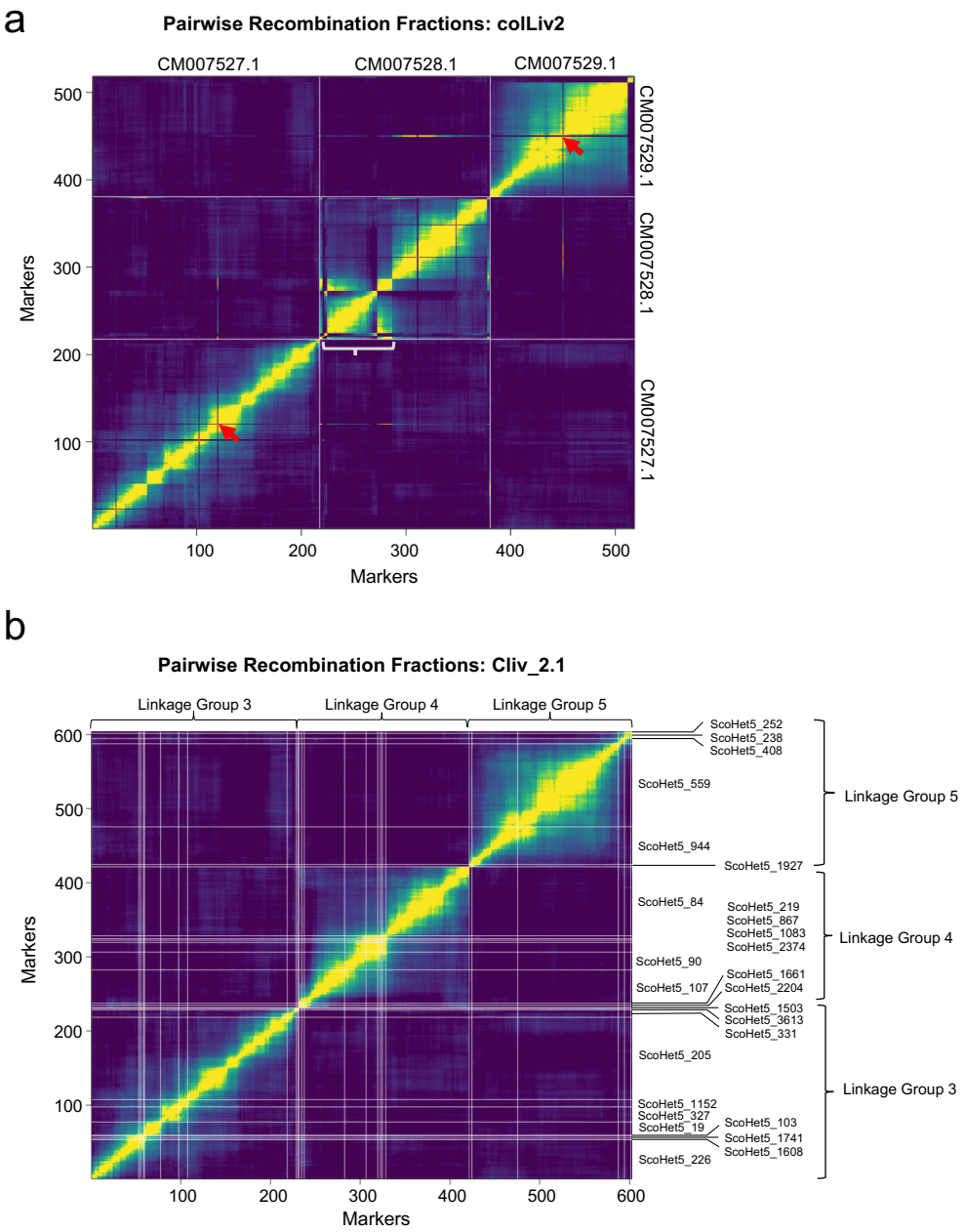

Figure 5. Correspondence between genotyping data and marker order in colLiv2 and Cliv_2.1 assemblies. (a) Representative plot of pairwise recombination fractions for GBS markers, ordered based on best alignment to colLiv2 assembly, for chromosomes CM007527.1, CM007528.1, and CM007529.1. X and Y axes show individual markers, ordered as they map to the colLiv2 chromosomes CM007527.1, CM007528.1, and CM007529.1. White lines mark the boundaries between chromosomes. Yellow indicates

569 low pairwise recombination fraction (linked markers), while purple indicates high
570 pairwise recombination fraction (unlinked markers). Red arrows highlight two markers,
571 one mapped to chromosome CM007527.1 and one mapped to CM007529.1, for which
572 recombination fractions suggest that these markers should instead be located on
573 chromosome CM007528.1. A white bracket indicates a region on chromosome
574 CM007528.1 where portions of the chromosome appear to be assembled in the wrong
575 order. (b) Plot of pairwise recombination fractions for the Cliv_2.1 scaffolds that make
576 up linkage groups 3, 4, and 5. In (a), colLiv2 CM007527.1 largely corresponds to linkage
577 group 3, CM007528.1 to linkage group 4, and CM007529.1 to linkage group 5. White
578 lines mark the boundaries between individual scaffolds, with scaffold IDs indicated on
579 the right side.

580 **TABLES**

581

Table 1. Assembly statistics for Cliv_2.1

Estimated Physical Coverage	389.7x
Total Length	1,108,534,737 bp
Total scaffolds	15,057
Total scaffolds >1kb	4,062
Total scaffolds >10kb	848

582

583

Table 2. Assembly version comparison

	Cliv_1.0	Cliv_2.1
Total Length	1110.8 Mb	1110.9 Mb
N50 Length	3.15 Mb and 82 scaffolds	14.3 Mb and 17 scaffolds
N90 Length	0.618 Mb and 394 scaffolds	1.56 Mb and 113 scaffolds
Completeness Estimate	72.3-86.4%	72.9-86.2%

584

585

586

587 **Table 3. Transcriptome assembly summary**

SRA accession	Tissue	Breed	# assembled transcripts
SRR521357	Heart	Danish tumbler	79473
SRR521358	Liver	Danish tumbler	35691
SRR521359	Heart	Oriental frill	71078
SRR521360	Liver	Oriental frill	74180
SRR521361	Heart	racing homer	80034
SRR521362	Liver	racing homer	80642
SRR5878849	Embryo	racing homer	208682
SRR5878850	Embryo	parlor roller	344735
SRR5878851	Spleen	racing homer	156415
SRR5878852	Olfactory epithelium	racing homer	112632
SRR5878853	Subepidermis	racing homer	185484
SRR5878854	Cochlear duct	racing homer	189438
SRR5878855	Brain	racing homer	131999
SRR5878856	Retina	racing homer	186060

588

589
590

591

Table 4. Annotation statistics for Cliv_2.1

	Genes	Transcripts
Total	15,392	18,966
match[a]	14,898	18,472
new	494	494

[a] Count that match Cliv_1.0 annotations with a value of at least 90% (match is calculated as % identity multiplied by % end-to-end coverage)

592

Table 5. Annotation version comparison

	Cliv_1.0	Cliv_2.1
Total Gene Models	15,724	15,392
coding	15,022	14,683
non-coding	702	709
Total Transcripts	19,585	18,966
coding	18,569	18,148
non-coding	1016	818

593

594

595 **Table 6. Summary of Cliv_2.1 alignment to colLiv2 chromosome-level scaffolds.** Overall,
596 colLiv2 appears to exclude 1,184, or approximately 7.7%, of the 15,392 annotated genes from the
597 Cliv_2.1 assembly; this is consistent with the overall decrease in genome size.
598

Cliv_2.1 scaffold representation	# of scaffolds	Scaffold length range	Scaffolds with genes	# of genes	Genes in LAST alignment to colLiv2	Genes missing from LAST alignment to colLiv2
Missing	14,189	200-393,647	147	164	NA	164
≤50% aligned	251	318-2,545,801	183	506	369	137
50-75% aligned	183	581-5,717,624	251	638	550	88
≥75% aligned	434	259-94,473,889	434	14,084	13,289	795

599
600

601 **SUPPLEMENTAL TABLES**

602

603 **Table S1. Positions of Cliv_1.0 scaffolds in the Cliv_2.1 scaffolds.** The table has the
604 following format: column 1, Cliv_2.1 scaffold name; column 2, Cliv_1.0 sequence name; column
605 3, starting base (zero-based) of the Cliv_1.0 sequence; column 4, ending base of the Cliv_1.0
606 sequence; column 5, orientation of the Cliv_1.0 sequence in the Cliv_2.1 scaffold, where (-)
607 indicates that the Cliv_2.1 scaffold sequence is reverse complemented relative to the Cliv_1.0
608 assembly; column 6, starting base (zero-based) in the Cliv_2.1 scaffold; column 7, ending base in
609 the Cliv_2.1 scaffold.

610

611 **Table S2. Positions of breaks made in the Cliv_1.0 assembly to create the Cliv_2.1**
612 **assembly**. Data fields follow the same format that is used in Supplemental Table 1.

613

614 **Table S3. Summary of transposable element fragments, parsed into 1 My bins based on**
615 **substitution rate**

616

617 **Table S4. Summary information of repeat masking, by class and by family**

618

619 **Table S5. Transcript count and cumulative distribution function (CDF) binned by**
620 **Annotation Edit Distance (AED) values**. AED is a modified sensitivity/specificity metric used to
621 compare annotation datasets to each other or to aligned transcriptome and protein homology
622 datasets. For calculating AED, sensitivity is defined as the fraction of a given reference
623 overlapping a prediction and measures false negative rates. For our purposes, the prediction is a
624 transcript model and the reference (or truth set) is a set of aligned transcriptome and protein
625 homology evidence. We calculate sensitivity using the formula $SN = |p \cap r|/|r|$; where $|p \cap r|$
626 represents the number overlapping nucleotides between the prediction and reference, and $|r|$
627 represents the total number of nucleotides in the reference. Specificity is then defined as the
628 fraction of a prediction overlapping a given reference, and it measures false positive rates. We

629 calculate specificity using the formula SP = |p∩r|/|p|. We then define concordance to be the
630 average of sensitivity and specificity (C = (SN+SP)/2), and AED is 1 minus the concordance (AED
631 = 1- C). Transcript models that have high AED values then show little concordance to aligned
632 experimental evidence, and models with low AED values show high concordance.
633
634 **Table S6. Linkage map assembled from genotype-by-sequencing markers aligned to the**
635 **Cliv_2.1 assembly, and positions of aligned markers within the Cliv_2.1, Cliv_1.0, and**
636 **colLiv2 assemblies**.
637
638 **Table S7. Summary of GBS markers for which best BLAST alignment to colLiv2 is**
639 **discordant with linkage data.** Columns describe marker position in the linkage map, the best
640 BLAST hit within the colLiv2 assembly, and the marker position in the Cliv_2.1 assembly. For
641 each marker, the colLiv2 chromosome to which the marker appears to be linked is also indicated.